

Internal Fault Classification in Transformer Windings using Combination of Discrete Wavelet Transforms and Back-propagation Neural Networks

Atthapol Ngaopitakkul and Anantawat Kunakorn*

Abstract: This paper presents an algorithm based on a combination of Discrete Wavelet Transforms and neural networks for detection and classification of internal faults in a two-winding three-phase transformer. Fault conditions of the transformer are simulated using ATP/EMTP in order to obtain current signals. The training process for the neural network and fault diagnosis decision are implemented using toolboxes on MATLAB/Simulink. Various cases and fault types based on Thailand electricity transmission and distribution systems are studied to verify the validity of the algorithm. It is found that the proposed method gives a satisfactory accuracy, and will be particularly useful in a development of a modern differential relay for a transformer protection scheme.

Keywords: Discrete wavelet transforms, internal faults, neural network, transformer windings.

1. INTRODUCTION

Protective devices are an important part for detecting fault conditions in a power system. The appropriate protection scheme must be selected to ensure the safety of power apparatus and reliability of the system. Generally, power transformers can be protected by overcurrent relays, pressure relays and differential relays depending on purposes [1]. For differential protection, the differential current, which is generated by a comparison between the primary current and the secondary current detected via current transformers, is required. The differential protection is aimed at detecting internal faults in transformer windings. In a normal operation or in a fault condition due to the external short circuits, the differential current is relatively small, and the differential relay should not function [1,2]. However, there are some factors that can cause a needless operation of the differential protection such as effects from magnetizing inrush current. To avoid the malfunction of the differential relay, the discrimination between internal faults, magnetizing inrush current and external short circuit current is required [1-3]. Several transformer models and decision algorithms have been proposed and discussed for such a task [4-6]. Recently, with the advance of signal processing technologies

and artificial intelligent tools, the development of more sophisticated protection systems as well as fault diagnosis for the power transformer has been progressed with the applications of wavelet transform (WT) and artificial neural networks (ANNs) [7-10].

This paper presents an application of Wavelet transform and a decision algorithm based on back propagation neural networks in order to detect the internal faults at the windings of a two-winding transformer. The transformer model with the stray capacitances is used so that internal fault signals with high frequency components can be calculated. The simulations, analysis and diagnosis are performed using ATP/EMTP and MATLAB. The current waveforms obtained from ATP/EMTP are extracted to several scales with the Wavelet transform, and the coefficients of the first scale from the Wavelet transformer are investigated. The comparison of the coefficients is performed and used as an input for training processes of the neural networks. The construction of the decision algorithm is detailed and implemented with various case studies based on Thailand electricity transmission and distribution systems.

2. WAVELET TRANSFORMS

Normally, the traditional method of signal analysis is based on Fourier transforms. Fourier transform is a process of multiplying a signal by a sinusoid in order to determine frequency contents of a signal. The output of the Fourier transform is sinusoids of different frequencies. It is found that Fourier transform is not appropriate to analyse faults in a power system with transient based protection methods,

Manuscript received August 30, 2005; accepted February 7, 2006. Recommended by Editorial Board member Yuan Fang Zheng under the direction of Editor Jin Young Choi.

Atthapol Ngaopitakkul and Anantawat Kunakorn are with Department of Electrical Engineering, Faculty of Engineering, King Mongkut's Institute of Technology Ladkrabang, Bangkok 10520, Thailand (e-mail: kkananta@kmitl.ac.th).

* Corresponding author.

because in such a system the desirable information may be located in both the frequency domain and the time domain. Due to the limits of Fourier transforms in applications with transient signals, Wavelet transforms has been proposed as an alternative tool in signal analysis. A wavelet is a small-localized wave of a particular shape and finite duration that has an average value of zero. The wavelet transform is a tool that cuts up data or functions or operators into different frequency components, and then studies each component with a resolution matched to its scale [11, 12]. The advantage of the transform is that the band of analysis can be fine adjusted so that high frequency components and low frequency components are detected precisely. Results from the wavelet transform are shown on both the time domain and the frequency domain. The wavelet transform can expand signals in term of using a shift in time or translation as well as compression in time or dilation of a fixed wavelet function named as the mother wavelet [9]. The wavelet transform, which has a change in the analysis scaled by the factor of two, is called discrete wavelet transform (DWT) as in (1).

$$DWT(m,n) = \frac{1}{\sqrt{2^m}} \sum_k f(k) \psi \left[\frac{n - k2^m}{2^m} \right], \quad (1)$$

where $\psi \left[\frac{n - k2^m}{2^m} \right]$ = mother wavelet (in this paper, Daubechies 4 is selected as a mother wavelet.)

3. TRANSFORMER WINDING MODELS

For a computer model of a two-winding three-phase transformer having primary and secondary windings in each phase, BCTRAN is a well-known subroutine on ATP/EMTP. To study internal faults of the transformer, Bastard et al proposed modification of the BCTRAN subroutine. Normally, the BCTRAN uses a matrix of inductances with a size of 6x6 to represent a transformer, but with the internal fault conditions the matrix is adjusted to be a size of 7x7 for winding to ground faults and of 8x8 for interturn faults [4]. In the research work of Bastard et al [4], the model was proved to be validate and accurate due to a comparison with measurement results. However, the effects of high frequency components which may occur during the faults are not included in such a model. Islam and Ledwich [5] described the characteristics of high frequency responses of a transformer due to various faults. It has been shown that the fault types and fault locations have an influence on the frequency responses of the transformer [5]. In addition, it has been proved that transient based protections using high frequency components in fault currents can be applicable in

locating and classifying faults on transmission lines [13,14]. It is, therefore, useful to investigate the high frequency components superimposed on the fault current signals for a development of a transient based protection for a transformer. As a result, in this paper the combination of the transformer models proposed by Bastard et al [4] as shown in Fig. 1, with the high frequency model including capacitances of the transformer recommended by IEEE working group [15] as shown in Fig. 2, are used for simulations of internal faults at the transformer windings.

From Fig. 1, for the phase winding of the transformer with internal faults, the winding is divided into two parts in the case of winding to ground faults, and three parts in the case of interturn faults.

The capacitances shown in Fig. 2 are as follows:

C_{hg} = stray capacitance between the high voltage winding and ground

C_{lg} = stray capacitance between the low voltage winding and ground

C_{hl} = stray capacitance between the high voltage winding and the low voltage winding.

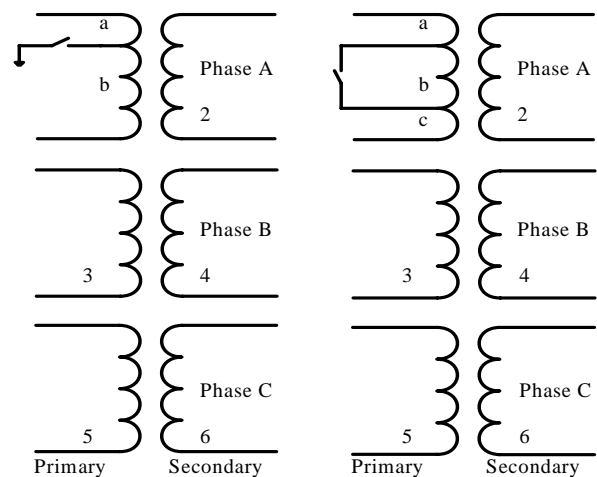


Fig. 1. The modification on ATP/EMTP model for a three-phase transformer with internal faults[4].

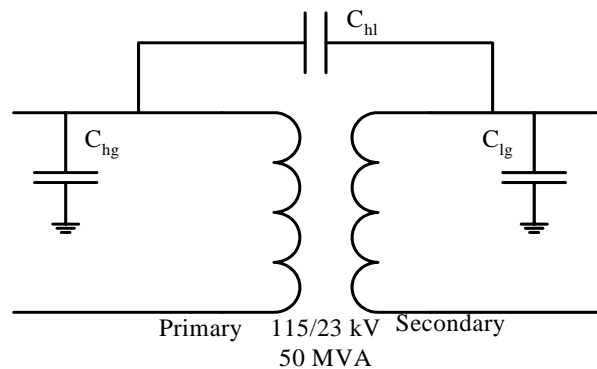


Fig. 2. A two-winding transformer with the effects of stray capacitances[15].

4. CASE STUDIES AND FAULT DETECTION ALGORITHMS

A 50 MVA, 115/23 kV two-winding three-phase transformer was employed in simulations with all parameters and configuration provided by a manufacturer [16]. The scheme under investigations is a part of Thailand electricity transmission and distribution system as depicted in Fig. 3. It can be seen that the transformer as a step down transformer is connected between two subtransmission sections. The primary and secondary current waveforms, then, can be simulated using ATP/EMTP, and these waveforms are imported into MATLAB/Simulink for a construction of fault diagnosis process.

To implement the transformer model and cover all regions of operating conditions training and testing data were simulated with various changes in system parameters as follows:

- The angles on phase A voltage waveform for the instants of fault inception were 30° and 210° .
- Two types for internal faults at the transformer windings (both primary and secondary) which are winding to ground faults and interturn faults, were investigated.
- For the winding to ground faults, the fault locations were designated on any phases of the transformer windings (both primary and secondary) at the length of 10%, 20%, 30%, 40%, 50%, 60%, 70%, 80% and 90% measured from the line end of the windings.
- For the interturn faults, the position of point a on the transformer winding, as shown in Fig. 1, was varied at the length of 10%, 20%, 30%, 40%, 50%, 60%, 70% and 80% measured from the line end of the windings.
- For the interturn faults, the position of point b on the transformer winding, as shown in Fig. 1, was varied at the length of 10%, 20%, 30%, 40%, 50%, 60%, 70% and 80% measured from the line end of the windings.
- Fault resistance was 5Ω .

With fault signals obtained from the simulations, the differential currents, which are a deduction between the primary current and the secondary current in all three phases as well as the zero sequence, are calculated, and the resultant current signals are extracted using the Wavelet transform. The coefficients of the signals obtained from the Wavelet transform are squared for a more explicit comparison. Fig. 4 illustrates an example of an extraction using Wavelet transform for the differential currents and zero sequence current from scale1 to scale 5 for a case of phase A to ground fault at 40% in length of the high voltage winding.

After applying the Wavelet transform to the differential currents, the comparison of the coefficients from each scale is considered so that the fault classifications can be analysed. In case of internal faults and external faults Wavelet transform is

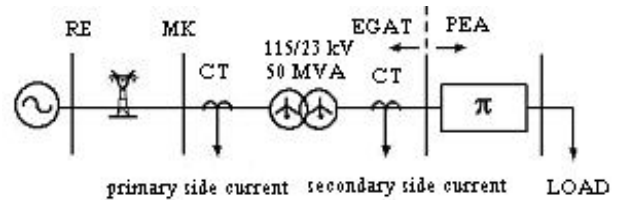


Fig. 3. The system used in simulations studies.

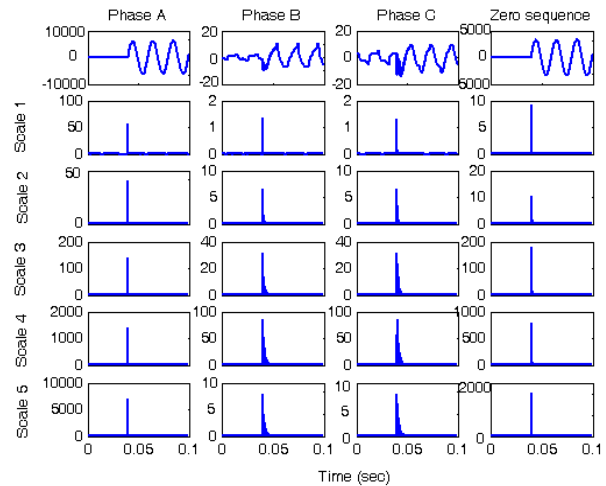


Fig. 4. Wavelet transform of differential currents (Turn to ground fault at 40% in length of the high voltage winding).

applied to the quarter cycle of current waveforms after the fault inception. With several trial and error processes, the decision algorithm on the basis of computer programming technique is constructed. The most appropriate algorithm for the decision with all results from the case studies of the system under the investigations can be concluded as follows[17]:

For detecting the phase with a fault condition, for $t_d = 0.000005 : 0.000005 : 0.1$

```

if      (  $X_{(td+t1)}^{diff} \geq 5 * X_{max(0 \rightarrow td)}^{diff}$  )
      then       $X_{chk}^{diff} = 1$ 
      else
               $X_{chk}^{diff} = 0$ 
      end
end
    
```

where

$t1 = 5 \mu\text{sec}$ (depending on the sampling time used in ATP/EMTP),

$X_{(td+t1)}^{diff}$ = coefficient from Wavelet transform for the differential current detected from phase X at the time of $td+t1$,

$X_{max(0 \rightarrow t)}^{diff}$ = coefficient from Wavelet transform for the

differential current detected from phase X at the time from $t=0$ to $t=td$,

X_{chk}^{diff} = comparison indicator for a change in coefficient from Wavelet transform ($A_{check}^{diff}, B_{check}^{diff}, C_{check}^{diff}$), used for separation between normal conditions and faults.

By performing many simulations, it has been found that when applying the previously detailed algorithm for detecting internal faults at the transformer winding, the coefficient in scale 1 from DWT seems enough to indicate the internal fault inception of the transformer. As a result, it is unnecessary to use other coefficients from higher scales in this algorithm, and the coefficients in scale 1 from DWT are used in training processes for the neural networks later.

5. NEURAL NETWORK DECISION ALGORITHM AND SIMULATION RESULTS

Artificial neural networks are an attempt to simulate the human brain's non-linear and parallel processing capabilities. Although there are many types of neural networks, only a few of neuron-based structures are being used commercially. One particular structure, a back-propagation neural network, is the most popular tool for applications such as pattern recognition fault classification etc. A structure of a back propagation neural network consists of three layers which are an input layer, at least one hidden layer and an output layer. Each layer is connected with weights and bias. In this paper, a three-layer back propagation neural network with one input layer, two hidden layers and one output layer is employed as shown in Fig. 5.

Hyperbolic tangent sigmoid functions are used as an activation function in all hidden layers while linear function is used as an activation function in output layers. In addition, there are many adjustment weight and bias in the neural network toolbox such as quasi-

Newton algorithm, Levenberg-Maquardt algorithm, Resilient Backpropagation, Conjugate Gradient algorithm etc. Each method has difference efficiency and training time. A comparison of the various training algorithms has been mentioned, and it is shown that Levenberg-Marquardt algorithm has the fastest convergence [18]. As a result, Levenberg-Marquardt algorithm is selected as adjustment weight and bias in this paper. A training process for the back propagation neural network can be divided into three parts as follows [18]:

- 1) The feedforward input pattern, which has a propagation of data from the input layer to the hidden layer and finally to the output layer for calculating responses from input patterns illustrated in (2) and (3).

$$a^2 = f^2(lw^{2,1} * f^1(iw^{1,1} * p + b^1) + b^2), \quad (2)$$

$$o / p_{ANN} = f^3(lw^{3,2} * a^2 + b^3), \quad (3)$$

where

p = input vector of ANNs,

$iw^{1,1}$ = weights between input and the first hidden layer,

$lw^{2,1}$ = weights between the first and the second hidden layers,

$lw^{3,2}$ = weights between the second hidden layer and output layers,

b^1, b^2 = bias in the first and the second hidden layers respectively,

b^3 = bias in output layers,

f^1, f^2 = activation function(Hyperbolic tangent sigmoid function : \tanh),

f^3 = activation function(Linear function).

- 2) The back-propagation for the associated error between outputs of neural networks and target outputs; The error is fed to all neurons in the next lower layer, and also used to an adjustment of weights and bias.

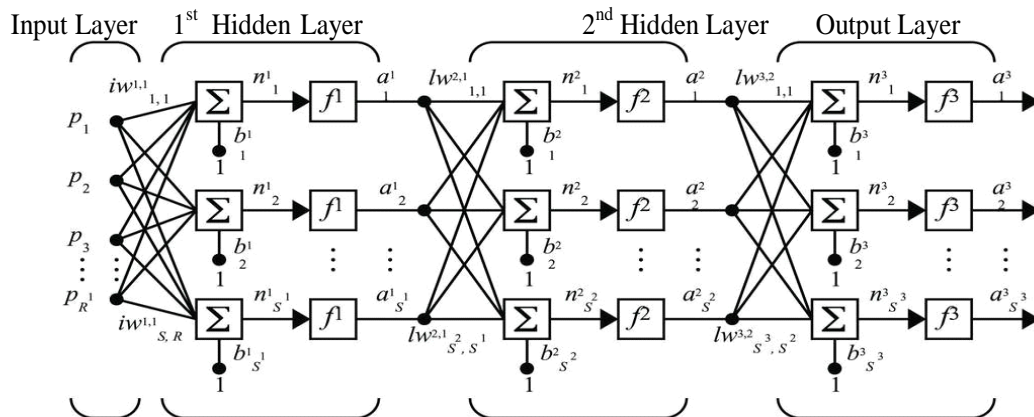


Fig. 5. Back propagation with two hidden layers [18].

3) The adjustment of the weights and bias by Levenberg-Marquardt (trainlm). This process is aimed at trying to match between the calculated outputs and the target outputs. Mean absolute percentage error (MAPE) as an index for efficiency determination of the back-propagation neural networks is computed in (4).

$$MAPE = \frac{1}{n} * \sum_{i=1}^n \left| \frac{o/P_{ANNi} - o/P_{TARGETi}}{o/P_{TARGETi}} \right| * 100\% , (4)$$

where n = number of test sets.

A training process was performed using neural network toolboxes in MATLAB [18]. A structure of the back propagation neural network consists of 4 neuron inputs and 8 neuron outputs. The inputs are the maximum coefficients of the differential currents and zero sequence current as mentioned in the previous section. In this paper, there are 360 sets for training. The output variables of the neural networks are designated as either 0 or 1 with various types of faults as shown in Table 1.

Before starting the training process, a number of neurons in each hidden layer have to be fixed according to various factors such as: number of input

Table 1. Output patterns from neural networks for various fault types.

| Classifications of Fault | A1 | B1 | C1 | G1 | A2 | B2 | C2 | G2 |
|--------------------------------|----|----|----|----|----|----|----|----|
| Winding to ground phase A (HV) | 1 | 0 | 0 | 1 | 0 | 0 | 0 | 0 |
| Winding to ground phase A (LV) | 0 | 0 | 0 | 0 | 1 | 0 | 0 | 1 |
| Interturn phase A (HV) | 1 | 0 | 0 | 0 | 0 | 0 | 0 | 0 |
| Interturn phase A (LV) | 0 | 0 | 0 | 0 | 1 | 0 | 0 | 0 |
| Winding to ground phase B (HV) | 0 | 1 | 0 | 1 | 0 | 0 | 0 | 0 |
| Winding to ground phase B (LV) | 0 | 0 | 0 | 0 | 0 | 1 | 0 | 1 |
| Interturn phase B (HV) | 0 | 1 | 0 | 0 | 0 | 0 | 0 | 0 |
| Interturn phase B (LV) | 0 | 0 | 0 | 0 | 0 | 1 | 0 | 0 |
| Winding to ground phase C (HV) | 0 | 0 | 1 | 1 | 0 | 0 | 0 | 0 |
| Winding to ground phase C (LV) | 0 | 0 | 0 | 0 | 0 | 0 | 1 | 1 |
| Interturn phase C (HV) | 0 | 0 | 1 | 0 | 0 | 0 | 0 | 0 |
| Interturn phase C (LV) | 0 | 0 | 0 | 0 | 0 | 0 | 1 | 0 |

and output neurons, number of training cases and the type of activation function in hidden layer etc. The initial number of neurons for the first hidden layer can be calculated as shown in (5).

$$z = \frac{2}{3}(r + q), (5)$$

where

z = Initial number of neurons in the first hidden layer,

r = Number of neurons input,

q = Number of neurons output.

When the initial number of neurons in the first hidden layer had been determined, the final number of the neurons in the same layer had to be calculated in order to stop the training process. The final number can be obtained from:

$$z_{st} = z + z1, (6)$$

where

z_{st} = the final number for the neurons in the first hidden layer,

$$z1 = \begin{cases} 5 & 2 \leq z \leq 6 \\ 4 & 7 \leq z \leq 10 \\ 3 & 11 \leq z \leq 13 \\ 2 & 14 \leq z \end{cases}$$

During the training process, the weight and biases were adjusted, and there were 20,000 iterations in order to compute the best value of MAPE. The number of neurons in both hidden layers was increased before repeating the cycle of the training process. The training procedure was stopped when reaching the final number of neurons for the first hidden layer or the MAPE of test sets was less than 0.5%. The training process can be summarized as a flowchart shown in Fig. 6 while various results from the training process can be shown in Table 2 with the initial number of neurons for the first hidden layer obtained from (5).

Table 2. Results from the training process (Performed on a PC with Pentium IV 2.4GHz CPU, with 512 MB RAM).

| Number of neurons in the first hidden layer | MAPE of Test set (%) | Time used in training process (minute) |
|---|----------------------|--|
| 8 | 0.55556961 | 100.59 |
| 9 | 0.5555649 | 141.28 |
| 10 | 0.59023954 | 178.32 |
| 11 | 0.5678628 | 221.12 |

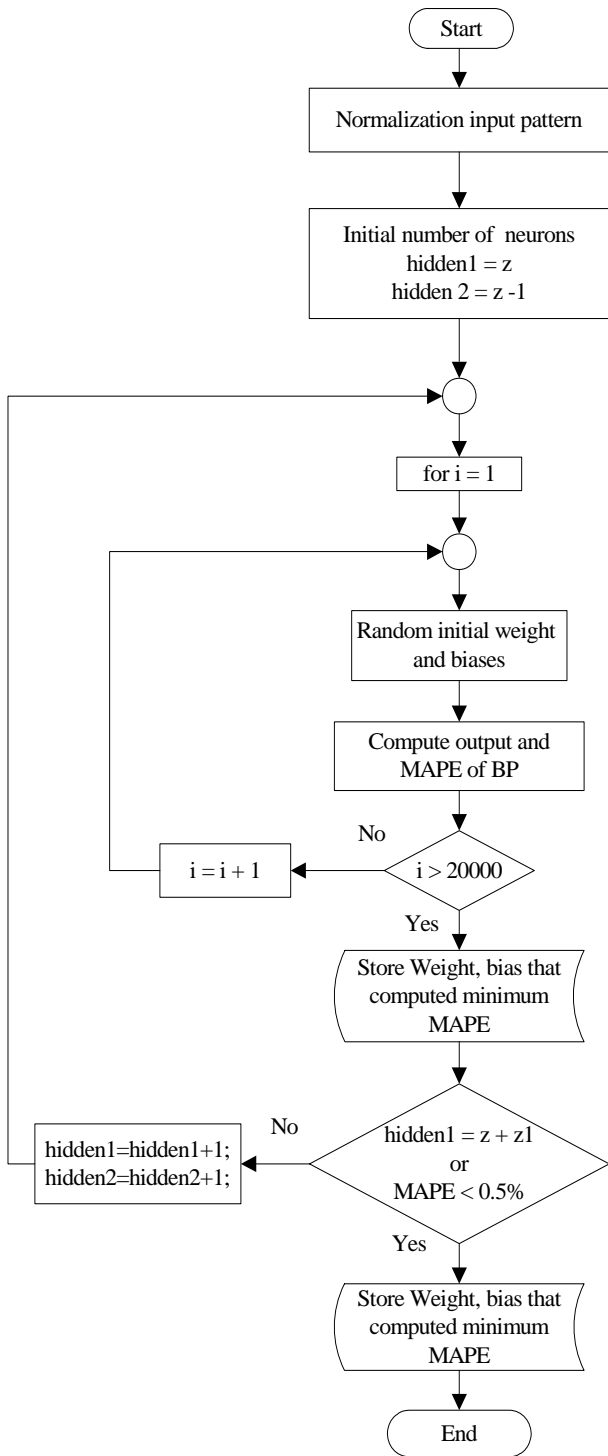


Fig. 6. Flowchart for the training process.

The decision algorithm based on the neural network, then, is tested with 180 case studies. The internal fault conditions in the windings of the transformer are simulated on ATP/EMTP. In order to explain the verification of the neural network algorithm, the simulation results shown in Fig. 4 are used as an example. For this case, when applying the decision algorithm for a prediction, the output obtained from neural network is as shown in Table 3.

Table 3. Outputs from the neural network for the simulation case shown in Fig. 4.

| | | | | | | | |
|----|----|----|----|----|----|----|----|
| A1 | B1 | C1 | G1 | A2 | B2 | C2 | G2 |
| 1 | 0 | 0 | 1 | 0 | 0 | 0 | 0 |

Table 4. Accuracy of fault classification from the proposed algorithm.

| Types of faults | Number of case studies | Accuracy |
|--|------------------------|----------|
| Winding to ground fault at the high voltage side | 18 | 100% |
| Winding to ground fault at the low voltage side | 18 | 100% |
| Interturn fault at the high voltage side | 72 | 98.61% |
| Interturn fault at the low voltage side | 72 | 100% |

From Table 3, it can be seen that the index value at A1 is 1 and that at G1 is also 1 while others are 0. This means that there is an internal fault occurring at the high voltage side, and the internal fault is classified as a winding to ground fault, which is correlative to the condition of the transformer used in simulations of Fig. 4.

In addition, when all case studies are tested with various types of internal faults and different locations on both primary windings and secondary windings at the three-phase transformer, the accuracy of the results obtained from the prediction from the neural network is illustrated in Table 4.

6. CONCLUSIONS

A technique using discrete wavelet transform in combination with back propagation neural networks in order to classify internal fault types of a three-phase transformer has been proposed. The maximum values from the first scale at 1/4 cycle of phase A, B, and C of post-fault differential current signals and zero sequence current obtained by the wavelet transform have been used as an input for the training process of a neural network in a decision algorithm with a use of the back propagation neural networks. Various case studies have been studied including the variation of fault inception angles, fault types and fault locations. The results have illustrated that the proposed algorithm is able to predict the internal faults at windings of a transformer with an accuracy of higher than 98%. This technique should be useful in the differential protection scheme for the transformer. The further work will be the improvement of the algorithm so that fault locations on the windings of the transformer can be identified.

REFERENCES

- [1] S. H. Horowitz and A. G. Phadke, *Power System Relaying*, John Wiley & Sons, Inc, 1992.
- [2] A. G. Phadke and J. S. Thorp, "A new computer-based flux restrained current-differential relay for power transformer protection," *IEEE Trans. on Power Apparatus and System*, vol. PAS-102, no. 11, pp. 3624-3629, November 1983.
- [3] T. S. Sidhu and M. S. Sachdev, "On-line identification of magnetizing inrush current and internal faults in three-phase transformers," *IEEE Trans. on Power Delivery*, vol. 7, no. 4, pp. 1885-1891, October 1992.
- [4] P. Bastard, P. Bertrand, and M. Meunier, "A transformer model for winding fault studies," *IEEE Trans. on Power Delivery*, vol. 9, no. 2, pp. 690-699, April 1994.
- [5] S. M. Islam and G. Ledwich, "Locating transformer faults through sensitivity analysis of high frequency modeling using transfer function approach," *Proc. of IEEE International Symposium on Electrical Insulation*, pp. 38-41, June 1996.
- [6] H. Wang and K. L. Butler, "Modeling transformers with internal incipient faults," *IEEE Trans. on Power Delivery*, vol. 17, no. 2, pp. 500-509, April 2002.
- [7] Y. Zhang, X. Ding, Y. Liu, and P. J. Griffin, "An artificial neural network approach to transformer fault diagnosis," *IEEE Trans. on Power Delivery*, vol. 11, no. 4, pp. 1836-1841, October 1996.
- [8] M. G. Morante and D. W. Nocolletti, "A wavelet-based differential transformer protection," *IEEE Trans. on Power Delivery*, vol. 14, no. 4, pp. 1352-1358, October 1999.
- [9] O. A. S. Youssef, "A wavelet-base technique for discrimination between faults and magnetizing inrush currents in transformers," *IEEE Trans. on Power Delivery*, vol. 18, no. 1, pp. 170-176, January 2003.
- [10] P. Purkait and S. Chakravorti, "Wavelet transform-based impulse fault pattern recognition in distribution transformers," *IEEE Trans. on Power Delivery*, vol. 18, no. 4, pp. 1588-1589, October 2003.
- [11] I. Daubechies, "The wavelet transform, time-frequency localization and signal analysis," *IEEE Trans. on Information Theory*, vol. 36, no. 5, pp. 961-1005, September 1990.
- [12] C. H. Kim and R. Aggarwal, "Wavelet transforms in power systems: Part I. General introduction to the wavelet transforms," *IEE Power Engineering Journal*, pp. 81-87, April 2000.
- [13] Z. Q. Bo, M. A. Redfern, and G. C. Weller, "Positional protection of transmission line using fault generated high frequency transient signals," *IEEE Trans. on Power Delivery*, vol. 15, no. 3, pp. 888-894, July 2000.
- [14] P. Makming, S. Bunjongjit, A. Kunakorn, S. Jiriwibhakorn, and M. Kando, "Fault diagnosis in transmission lines using wavelet transforms," *Proc. of IEEE Transmission and Distribution Conference*, Yokohama, Japan, pp. 2246-2250, October 2002.
- [15] IEEE working group 15.08.09 "Modeling and analysis of system transients using digital programs," *IEEE PES special publication*.
- [16] ABB Thailand, Test report no. 56039.
- [17] A. Ngaopitakkul, A. Kunakorn, and I. Ngamroo, "Discrimination between external short circuits and internal faults in transformer windings using discrete wavelet transforms," *Proc. of 40th IEEE Industries Application Society Annual Conference*, Hongkong, October 2005.
- [18] H. Demuth and M. Beale, *Neural Network Toolbox User's Guide*, The Math Work, March 2001.



Atthapol Ngaopitakkul graduated with B.Eng and M.Eng in electrical engineering from King Mongkut's Institute of Technology Ladkrabang, Bangkok, Thailand in 2002 and 2004 respectively. He is currently a Ph.D. candidate at the department of Electrical Engineering, King Mongkut's Institute of Technology Ladkrabang.

His research interests are on the applications of wavelet transform and neural networks in power system analysis.



Anantawat Kunakorn graduated with B.Eng (Hons) in electrical engineering from King Mongkut's Institute of Technology Ladkrabang, Bangkok, Thailand in 1992. He received his M.Sc in Electrical Power Engineering from University of Manchester Institute of Science and Technology, UK in 1996, and Ph.D. in Electrical

Engineering from Heriot-Watt University, Scotland, UK in 2000. He is currently an Associate Professor at the Department of Electrical Engineering, King Mongkut's Institute of Technology Ladkrabang, Bangkok, Thailand. He is a Member of IEEE and IEE. His research interest is electromagnetic transients in power systems.